MicroRNA-606 inhibits the growth and metastasis of triple-negative breast cancer by targeting Stanniocalcin 1

SUJIN CHOI[1*], HYUN-JU AN[1,2*], HYUN JEONG YEO[1], MIN-JI SUNG[1], JISU OH[3], KWANBUM LEE[4], SEUNG AH LEE[4], SEUNG KI KIM[4], JUNHAN KIM[1], ISAAC KIM[4] and SOONCHUL LEE[1,2]

[1]Department of Orthopedic Surgery, CHA Bundang Medical Center, CHA University School of Medicine, Seongnam, Gyeonggi 13488; [2]SL Bio, Inc., Pocheon, Gyeonggi 11160; [3]Division of Hemato-Oncology, Department of Internal Medicine, Yongin Severance Hospital, Yonsei University College of Medicine, Yongin, Gyeonggi 16995; [4]Department of General Surgery, CHA Bundang Medical Center, CHA University School of Medicine, Seongnam, Gyeonggi 13488, Republic of Korea

Abstract. Triple-negative breast cancer (TNBC) is associated with a poor prognosis; however, treatments for TNBC are limited, with poor outcomes. MicroRNAs (miRNAs/miRs) are small non-coding RNA molecules that are able to regulate gene expression. The present study aimed to identify differentially expressed miRNAs in patients with breast cancer, and to investigate the functional role of the identified miRNA targets and their effects *in vitro* and *in vivo*. Transfection with miR-606 suppressed TNBC cell proliferation, migration, invasion and tumor sphere-forming ability, as determined using trypan blue, Transwell and sphere formation assays. Moreover, miR-606 induced the apoptosis of TNBC cells, as determined by flow cytometric analysis. Furthermore, intratumoral injections of miR-606 mimics suppressed tumor growth in MDA-MB-231 xenografts. In addition, MDA-MB-231 cells transfected with miR-606 mimics exhibited decreased lung metastatic nodules in a mouse tail vein injection model. Notably, miR-606 and STC1 expression had opposing effects on the overall survival of patients with TNBC. The results of the present study suggested a novel tumor suppressor function for miR-606 in TNBC, thus indicating its potential application in the development of anticancer miRNA therapeutics.

Correspondence to: Professor Isaac Kim, Department of General Surgery, CHA Bundang Medical Center, CHA University School of Medicine, 335 Pangyo-ro, Bundang, Seongnam, Gyeonggi 13488, Republic of Korea
E-mail: isaac24@cha.ac.kr

Professor Soonchul Lee, Department of Orthopedic Surgery, CHA Bundang Medical Center, CHA University School of Medicine, 335 Pangyo-ro, Bundang, Seongnam, Gyeonggi 13488, Republic of Korea
E-mail: lsceline@cha.ac.kr

*Contributed equally

Introduction

Breast cancer is the most common type of cancer affecting women worldwide, with ~280,000 cases diagnosed annually (1). Breast cancer is classified as luminal A or B, human epidermal growth factor receptor 2 (HER2)-positive or -negative, and triple-negative or -positive according to the expression of hormone receptors and HER2 (2). Triple-negative breast cancer (TNBC) tumors lack expression of estrogen receptor (ER), progesterone receptor (PR) and HER2, have relatively poor outcomes, and cannot be treated with endocrine or HER2-targeted therapies (3).

MicroRNAs (miRNAs/miRs) constitute a large family of small non-coding RNAs comprised of 20-22 nucleotides that regulate target gene expression, mainly at the post-transcriptional level (4). Dysregulated miRNAs are involved in a broad spectrum of cellular processes in TNBC, exerting tumor-promoting or -suppressing effects depending on the cellular targets involved in tumor initiation, promotion, malignant conversion and metastasis (5). Notably, miRNAs have attracted considerable attention for their regulatory involvement in the initiation, progression and metastasis of breast cancer, and aberrant miRNA expression profiles have been reported in breast cancer (6).

Stanniocalcin 1 (STC1), which was first identified in bony fish, is a disulfide-bound glycoprotein hormone involved in plasma calcium and phosphate homeostasis (7). Previous studies have reported that STC1 functions as an oncogene in various types of cancer; for example, STC1 has been reported to promote metastasis in ovarian cancer and cancer-associated fibroblast-derived STC1 can promote stemness in hepatocellular carcinoma (8,9). Notably, STC1 promotes the growth and metastasis of breast cancer tumors (10,11). However, studies on STC1 function in TNBC are lacking. Therefore, understanding oncogenes and their regulators might be critical to developing potential antitumor therapeutics.

The Cancer Genome Atlas (TCGA) database comprises a collection of clinical data, DNA/RNA sequences and DNA methylation profiles of at least 500 cases of 20 different tumor types (12). The Gene Expression Omnibus (GEO) repository contains publicly available microarray, next-generation

sequencing and other forms of high-throughput functional genomic data (https://www.ncbi.nlm.nih.gov/geo) (13). The present study aimed to identify differential miRNA expression patterns in samples from patients with breast cancer using miRNA sequence expression profiles downloaded from TCGA and GEO. The present study identified hsa-miR-606 as a differentially expressed miRNA and investigated its tumor-suppressing role in TNBC cells. In addition, the targets of miR-606 and its effects on tumor growth in a mouse xenograft model were investigated, and its effects on metastasis were assessed in a mouse tail vein injection model.

Materials and methods

Cells, animals and reagents. The human TNBC cell lines HS 578T, BT20, MDA-MB-231 and BT549 were obtained from the Korean Cell Line Bank; Korean Cell Line Research Foundation, and have been authenticated in the past 3 years using a short tandem repeat analysis profile. The cells were cultured in Dulbecco's Modified Eagle Medium (DMEM; 1X; Welgene, Inc.) supplemented with 10% fetal bovine serum (Gibco; Thermo Fisher Scientific, Inc.) and penicillin-streptomycin (PS; 100 U/ml; Gibco; Thermo Fisher Scientific, Inc.). The human breast cancer cell lines T47D, SK-BR-3 and MCF7 were also obtained from the Korean Cell Line Bank; Korean Cell Line Research Foundation, and have been authenticated in the past 3 years using a short tandem repeat analysis profile. These cells were cultured in Roswell Park Memorial Institute 1640 (1X; Welgene, Inc.) supplemented with 10% fetal bovine serum and penicillin-streptomycin (100 U/ml). The human breast cell line MCF10A was obtained from the American Type Culture Collection, and was cultured in DMEM/Nutrient Mixture F12 (F12) (1X; Welgene, Inc.) supplemented with 10% fetal bovine serum and penicillin-streptomycin (100 U/ml). The cells were maintained at 5% CO_2 and 37°C in a humidified incubator, and were mycoplasma free.

Animal experimental procedures were reviewed and approved by the CHA University Animal Care and Use Committee (approval no. 210152; Seongnam, South Korea). A total of 32 female BALB/c nu/nu mice (age, 4 weeks, weight, 18-20 g) were purchased from Orient Bio, and were maintained at 23±1°C and 50±10% humidity under a 12-h light/dark cycle. Food and water were provided *ad libitum* under specific pathogen-free conditions.

G-Fectin and Lipofectamine® 3000 transfection reagents were purchased from Genolution, Inc. and Invitrogen; Thermo Fisher Scientific, Inc., respectively.

Acquisition of miRNA expression data. To investigate the expression of miRNAs in patients with breast cancer, a microarray dataset (GSE118782) was obtained from the publicly available GEO database (National Center for Biotechnology Information; https://www.ncbi.nlm.nih.gov/geo). The GSE118782 dataset includes RNA extracted from the plasma of 30 patients with breast cancer and 10 healthy control women; the levels of small noncoding RNA were quantitated using Affymetrix microarrays (14).

Cell transfection with RNA oligonucleotides. The miR-606 mimics and miR-606 inhibitor (anti-miR-606) were synthesized by Genolution, Inc. as an RNA duplex or as a 2'-O-methyl-modified oligoribonucleotide single strand with the following sequences: miR-606 mimics, 5'-AAACUACUG AAAAUCAAAGAU-3' and anti-miR-606, 5'-AUCUUUGAU UUUCAGUAGUUU-3'. The sequences were obtained from the miRBase database (version 22.1: https://www.mirbase.org). The sequences for the control miRNA and control anti-miRNA (Genolution, Inc.) are: 5'-CCUCGUGCCGUU CCAUCAGGUAGUU-3' or 5'-CAGUACUUUUGUGUAGUA CAA-3', respectively.

For transfection with miRNAs, MDA-MB-231 and BT549 cells at 30% confluence were transfected with the miRNAs at a final concentration of 40 nM for 48 h at 37°C using G-Fectin according to the manufacturer's instructions.

Tumor xenograft and lung metastasis experiments. To establish a tumor xenograft model, 5-week-old female BALB/c nu/nu mice were subcutaneously injected with MDA-MB-231 cells (10^7 cells in 100 μl PBS). Once the size of the tumor reached 150 mm^3, miRNA mimics were injected intratumorally, according to the manufacturer's protocol. Briefly, 10 μg miRNA mimics and 1.2 μl *in vivo*-jetPEI (Polyplus-transfection SA) were mixed at a volume of 50 μl, incubated for 15 min at room temperature and then injected into mice. To assess tumor size, the small diameter (SD) and large diameter (LD) of the tumor were measured twice a week using a Vernier caliper, and the tumor volume (V) was calculated using the equation: $V=(SD^2 \times LD) \times (\pi/6)$. At the endpoint, the mice were sacrificed in a CO_2 euthanasia chamber with a fill rate of 30% vol/min and the euthanasia of the mice was confirmed by a lack of breathing and faded eye color. The tumors were then collected for RT-qPCR and IHC analysis. In addition, to establish a lung metastasis model, MDA-MB-231 cells were transfected with miRNA mimics, resuspended at 4×10^5 cells in 200 μl PBS, and injected into the tail vein of mice after 48 h. Subsequently, the mice were sacrificed in a CO_2 euthanasia chamber with a fill rate of 30% vol/min at 6 weeks post-injection, and their lungs were collected. The dissected lungs were fixed in 3.7% paraformaldehyde for 10 min at 25°C and stained with Bouin's solution for 5 min at 25°C, after which the nodules formed in the lungs were counted.

Reverse-transcription quantitative (RT-q)PCR analysis. Total RNA was isolated from cultured cell lines (e.g., MCF10A, T47D, SK-BR-3, MCF7, HS 578T, BT20, MDA-MB-231 and BT549) or dissected xenograft tumor tissue using TRIzol® reagent (Invitrogen; Thermo Fisher Scientific, Inc.) according to the manufacturer's protocol. To quantify mRNA or miRNA expression, total RNA (1 μg) was reverse transcribed into cDNA using Maxime RT PreMix (oligo dT Primer; Intron Biotechnology, Inc.) or an HB miR Multi Assay Kit SYSTEM I (HeimBiotek, Inc.), respectively. The RT conditions of mRNA or miRNA were 45°C for 1 h and at 95°C for 5 min or 37°C for 1 h and 95°C for 5 min, respectively. Additionally, qPCR for mRNA or miRNA quantification was performed using AMPIGENE qPCR Green Mix Lo-ROX (Enzo Life Sciences, Inc.) or an HB miR Multi Assay Kit SYSTEM I (HeimBiotek, Inc.), respectively, in accordance with the manufacturers' instructions. The qPCR thermocycling conditions for detection of mRNA or miRNA expression levels

were Denaturation at 95°C for 2 min, followed by 40 cycles at 95°C for 5 sec and 60°C for 20 sec or denaturation at 95°C for 15 min, followed by 40 cycles at 95°C for 5 sec and 60°C for 40 sec, respectively. The mRNA expression levels were normalized to those of GAPDH, and the miRNA expression levels were normalized to those of RNU6B. The mRNA or miRNA expression levels were calculated using the $2^{-\Delta\Delta Cq}$ method (15). The sequences of the specific primers were as follows: Activin A receptor, type I (ACVR1), forward 5'-ACG TGGAGTATGGCACTATC-3', reverse 5'-CGACACACTCCA ACAGTGTA-3'; DCLRE1A, forward 5'-GTGGAGATGGTA TTCAGCAG-3', reverse 5'-CAGAAGACCATCAGGACA CT-3'; STC1, forward 5'-GACACAGTCAGCACAATCAG-3', reverse 5'-GAGGAGGACTTTCAGCTTCT-3'; GAPDH, forward 5'-GGAGCGAGATCCCTCCAAAAT-3', reverse 5'-GGCTGTTGTCATACTTCTCATGG-3', RNU6B, forward 5'-CTCGCTTCGGCAGCACA-3', reverse 5'-AACGCTTCA CGAATTTGCGT-3', and miR-606, forward 5'-AAACTACTG AAAATCAAA-3', reverse 5'-GATACAAGTGCCTGACCA CT-3'.

Cell counting assay. MDA-MB-231 and BT 549 cells were seeded in 6-well plates at 30% confluence and transfected with miRNA mimics. A total of 24, 48, 72 and 96 h post-trans-fection, cells were stained with trypan blue (Gibco; Thermo Fisher Scientific, Inc.) at 25°C for 5 min and were counted using a hemocytometer (NanoEntek, Inc.) and an Olympus CKX52 inverted light microscope (x100 magnification; Olympus Corporation).

Colony formation assay. MDA-MB-231 and BT549 cells were seeded in 60-mm dishes at a density of 500 cells/dish 48 h post-transfection with miRNA mimics. Thereafter, the dishes were incubated at 37°C in a humidified incubator containing 5% CO_2 for 2 weeks, and the medium was replaced with fresh medium every 4 days. Subsequently, the cells were rinsed once with PBS, fixed with 4% formaldehyde at 25°C for 10 min, washed in distilled water once and stained with 0.05% crystal violet solution at 25°C for 30 min, after which the colonies (>50 cells/colony) were counted.

Annexin V/PI apoptosis assay. MDA-MB-231 and BT549 cells were transfected with miRNA mimics in 6-well plates at 30% confluence. The apoptotic population in transfected cells was estimated by Annexin-FITC/PI double staining using the Annexin V-FITC Apoptosis Detection Kit I (BD Biosciences), according to the manufacturer's protocols. The stained cells were analyzed using a CytoFLEX Flow Cytometer (Beckman Coulter, Inc.) and CytExpert software version 2.4 (Beckman Coulter, Inc.).

Western blotting. MDA-MB-231 and BT549 cells were trans-fected with miRNA mimics using G-Fectin. Subsequently, the cells were collected in PBS in an Eppendorf tube and lysed with PRO-PREP™ Protein Extraction Solution (Intron Biotechnology, Inc.) to harvest the proteins. Subsequently, the protein concentrations were measured using the Pierce Bicinchoninic Acid Protein Assay Kit (Thermo Fisher Scientific, Inc.). Thereafter, 20 μg proteins were separated by SDS-PAGE on 8-12% gels at 100 V for 2 h and transferred onto PVDF membranes at 95 V for 2 h. After transfer, the membranes were blocked with 5% skim milk in Tris-buffered saline (TBS)-Tween 20 (TBST; Intron Biotechnology, Inc.) at room temperature for 1 h and incubated with specific primary antibodies in blocking solution overnight at 4°C. The specific primary antibodies were as follows: Anti-proliferating cell nuclear antigen (PCNA; cat. no. sc-25280, 1:1,000), anti-BAX (cat. no. sc-23959, 1:1,000), anti-fibronectin (cat. no. sc-8422, 1:1,000), anti-E-cadherin (cat. no. sc-8426, 1:1,000), anti-β-actin (cat. no. sc-47778, 1:1,000), and anti-STC1 (cat. no. sc-293435, 1:1,000) (all from Santa Cruz Biotechnology, Inc.); anti-cleaved-poly ADP ribose polymerase (PARP; cat. no. 9541, 1:1,000) and anti-cleaved-caspase 3 (cat. no. 9664, 1:1,000) (both from Cell Signaling Technology, Inc.); anti-DNA cross-link repair 1A (DCLRE1A; cat. no. A303-747A, 1:1,000; Bethyl Laboratories, Inc.; Thermo Fisher Scientific, Inc.); and anti-N-cadherin (cat. no. 610920, 1:1,000; BD Biosciences). The membranes were then washed three times with TBST every 10 min and incubated with HRP-conjugated anti-mouse IgG or anti-rabbit IgG secondary antibodies (cat. nos. A1012S and A1013S, 1:2,000; ACE BioLabs) and in TBST at room temperature for 2 h, followed by detection using a clear western ECL substrate (Bio-Rad Laboratories, Inc.).

Sphere formation assay. For sphere formation, cells were cultured in cancer stem cell (CSC)-like cell growth medium, which consisted of DMEM/F12 serum-free medium supple-mented with 2% B-27 (Gibco; Thermo Fisher Scientific, Inc.), 20 ng/ml Recombinant Human EGF (Gibco; Thermo Fisher Scientific, Inc.), and 20 ng/ml Recombinant Human FGFb (Gibco; Thermo Fisher Scientific, Inc.). The cells were seeded at 3,000 cells/well in 6-well ultra-low cluster plates (Corning Life Sciences) using CSC-like cell medium, cultured until the sphere size reached 50 μm, and transfected with the miRNA mimics at a final concentration of 100 nM using G-Fectin at 37°C. A total of 4 days post-transfection, images of the spheres were captured using an Olympus CKX52 inverted light micro-scope (x40 magnification), and the number and diameter of spheres were measured.

Wound healing assay. A wound healing assay was used to measure cell migration ability. Briefly, MDA-MB-231 and BT549 cells were transfected with miRNA mimics at ~100% confluence in 6-well plates. To create a straight wound, cell monolayers were scratched with a pipette tip and incubated with fresh serum-free medium. Images were captured at 0, 24 and 48 h after wounding using an Olympus CKX52 inverted light microscope (x100 magnification), and the wound area was measured using ImageJ 1.52a (National Institutes of Health).

Transwell assay. MDA-MB-231 and BT549 cells were transfected with miRNA mimics. For the invasion and migra-tion assays, the cells were suspended in serum-free DMEM and seeded at $5x10^4$ cells/well into the upper chamber of a Transwell plate (8.0-μm pore size; Corning Life Sciences), with or without Matrigel coating, respectively. For Matrigel coating, the upper chambers were incubated with Matrigel at 25°C for 30 min. The lower chambers were filled with DMEM supplemented with 10% FBS and 1% PS. After incubation for 60-72 h at 37°C, the migrated and invaded cells on the lower

surface of the filters were fixed for 3 min at 25°C in 100% methanol, stained for 5 min at 25°C in 0.05% crystal violet solution and then washed three times for 1 min in distilled water. Stained cells were counted using an Olympus CKX52 microscope (x200 magnification) in three randomly selected fields.

Selection of miR-606 putative target genes. Putative miR-606 target genes were predicted using the miRNA target prediction programs DIANA-MICROT version 4 (https://dianalab.e-ce. uth.gr/html/universe/index.php?r=microtv4), TargetScan release 8.0 (https://www.targetscan.org), and miRDB version 6.0 (http://www.mirdb.org). The common genes from all three algorithms were selected to obtain specific candidate genes.

Luciferase reporter assay. The possible binding sites of miR-606 in the human STC1 3'-UTR were predicted using the miRNA target prediction program TargetScan (https://www.targetscan.org). The four 3'-UTR fragments containing the putative miR-606 binding site (STC1 3'-UTR-1, STC1 3'-UTR-2, STC1 3'-UTR-3, and STC1 3'-UTR-4) were cloned into a pGL3UC vector (provided by V.N. Kim, Seoul National University, Seoul, South Korea) by Macrogen, Inc. MDA-MB-231 and BT549 cells were seeded in 24-well plates ($5x10^4$ cells/well) and incubated for 24 h, after which the cells were co-transfected with the reporter plasmid or empty pGL3UC (100 ng), *Renilla* plasmid (100 ng) and miR-606 (40 nM) for 48 h at 37°C using Lipofectamine 3000. A total of 48 h post-transfection, the transfected cells were lysed using 1X Passive Lysis Buffer (Promega Corporation) to obtain the release of the firefly and *Renilla* luciferase reporter enzymes into the cell lysate, and then the luciferase activity of the lysed cells was measured using a Dual-Luciferase Reporter Assay System (Promega Corporation) according to the manufacturer's protocol. The relative firefly luciferase activity was normalized to *Renilla* luciferase activity.

ELISA. STC1 protein concentrations were determined in the supernatants of MDA-MB-231 and BT549 cells transfected with miRNA mimics using a Human Stanniocalcin 1/STC ELISA Kit (Abcam, cat. no. ab213829). The cell culture supernatant was obtained via centrifugation of cells at 400 x g for 10 min at 4°C. STC1 concentration was measured using an Epoch Microplate Spectrophotometer (BioTek Instruments, Inc.) according to the manufacturer's protocol.

IHC analysis. For the IHC analysis of resected tumor tissues, a ready-to-use IHC/ICC kit (cat. no. K405-50; BioVision Inc.) was used according to the manufacturer's protocol. Briefly, tumor tissues were fixed with 3.7% paraformaldehyde for 24 h at 25°C and embedded in paraffin. The paraffin-embedded tumor tissue sections (5 μm) were then deparaffinized with xylene, rehydrated gradually in ethanol and microwaved for antigen retrieval in Antigen Retrieval Buffer (cat. no. ab93678; Abcam). Endogenous peroxidase activity was blocked in 3% hydrogen peroxide for 30 min at 25°C and sections were then incubated with blocking buffer (BioVision, Inc.) for 15 min at 25°C. Thereafter, the slides were washed with PBS and incubated with specific primary antibodies overnight at 4°C.

The following primary antibodies were used: Anti-STC1 (cat. no. LS-B14899, 1:200; LifeSpan BioScience), anti-PCNA (1:2,000), anti-BCL-2 (cat. no. sc-7382, 1:100; Santa Cruz Biotechnology, Inc.) and anti-BAX (1:100). Next, the slides were incubated with horseradish peroxidase-conjugated anti-mouse or anti-rabbit IgG polyclonal antibodies (cat. no. K405-50-4; BioVision Inc.) for 20 min at 25°C, washed with PBS and were subsequently developed by staining with 3,3'-diaminobenzidine for 10 min at 25°C. For H&E staining, tumor or lung tissue was fixed with 3.7% paraformaldehyde for 24 h at 25°C and embedded in paraffin. The paraffin-embedded tumor or lung tissue sections (5 μm) were then deparaffinized with xylene and rehydrated gradually in ethanol. The sections were incubated with hematoxylin solution (cat. no. 03971; MilliporeSigma) for 5 min, washed twice with distilled water, incubated with eosin solution (cat. no. 318906; MilliporeSigma) for 3 min, and then washed with ethanol. Images were captured using the ZEISS Axioscan 7 microscope in brightfield scanning mode (Zeiss GmbH).

Overall survival (OS) analysis. To examine the association between OS and miR-606 or STC1 expression, survival analysis was performed using the K-M plotter database (www. kmplot.com; accessed on August 4, 2022) (16). The parameters were set in the Breast cancer miRNA database of the K-M plotter program as follows: i) Select a dataset, TCGA; ii) gene symbol, hsa-miR-606; iii) divided patients by auto-selecting the best cutoff; iv) survival, OS; v) molecular subtype, TNBC. The parameters were set in the Breast cancer mRNA database of the K-M plotter program as follows: i) gene symbol, STC1; ii) divided patients by auto-selecting the best cutoff; iii) survival, OS; iv) ER status, PR status, HER2 status, negative; v) subtype, basal.

Statistical analysis. All statistical analyses were performed using GraphPad Prism Software 8 (Dotmatics). Comparisons between groups were evaluated using the one-way analysis of variance with Tukey's post hoc test or unpaired Student's t-test. Data are presented as the mean ± standard error of the mean. For in vitro analyses, experiments were performed in triplicate. $P<0.05$ was considered to indicate a statistically significant difference.

Results

miR-606 induces the apoptosis of TNBC cells. The present study first investigated the miRNAs that could regulate breast cancer cell proliferation. The expression profiles of human miRNAs from a GEO dataset (GSE118782) revealed that miR-606 was downregulated in the plasma of patients with breast cancer (Fig. S1A). Furthermore, miR-606 expression levels were lower in TNBC cells (i.e., HS 578T, BT20, MDA-MB-231 and BT549) compared with those in normal breast cells or in cell lines of other breast cancer subtypes (i.e., MCF10A, T47D, SK-BR-3 and MCF7) (Fig. S1B). To determine the functional roles of miR-606 in tumor growth inhibition, the TNBC cell lines MDA-MB-231 and BT549 with the lowest miR-606 expression (Fig. S1B) were transfected with miR-606 mimics. Transfection efficacy was confirmed using RT-qPCR analysis, which showed that
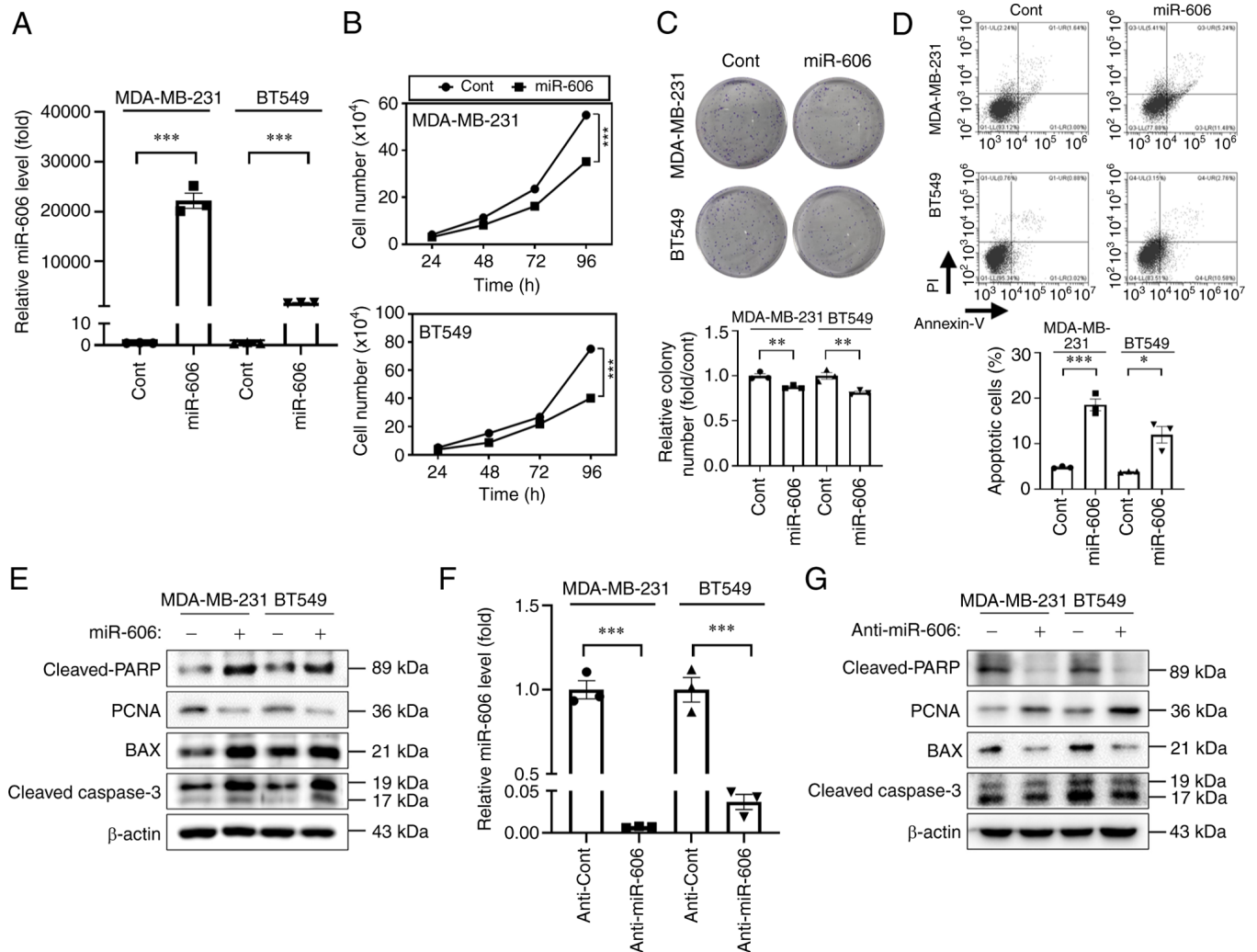
Figure 1. miR-606 induces the apoptosis of TNBC cells. (A) RT-qPCR analysis of miR-606 expression levels in TNBC cells transfected with miR-606 mimics. (B) Number of miR-606 mimics-transfected TNBC cells per well (in 6-well plates) at the indicated times. (C) Representative images of colony formation and relative number of colonies of TNBC cells transfected with miR-606 mimics. (D) Analysis of apoptotic TNBC cells transfected with miR-606 mimics using Annexin V/PI staining. (E) Western blot analysis of the relative expression levels of proteins related to the proliferation and apoptosis of TNBC cells transfected with miR-606 mimics. (F) RT-qPCR analysis of miR-606 expression levels in TNBC cells transfected with anti-miR-606. (G) Western blot analysis of the relative expression levels of proteins related to the proliferation and apoptosis of TNBC cells transfected with anti-miR-606. Data are presented as the mean ± SEM and were analyzed using Student's t-test. $^*P<0.05$, $^{**}P<0.005$ and $^{***}P<0.001$. TNBC, triple-negative breast cancer; Cont, control; miR, microRNA; PARP, poly ADP ribose polymerase; PCNA, proliferating cell nuclear antigen; RT-qPCR, reverse transcription-quantitative PCR.

miR-606 expression levels were significantly increased after transfection for 48 h compared with after transfection for 0 h with miR-606 mimics (Fig. S2). In addition, as shown in Fig. 1A, the expression levels of miR-606 were significantly increased in cells transfected with miR-606 mimics compared with in those transfected with the control miRNA for 48 h. The proliferation-inhibiting activity of miR-606 was confirmed by counting the number of cells at different time points post-transfection; miR-606 overexpression significantly suppressed the proliferation of MDA-MB-231 and BT549 cells (Fig. 1B). Colony formation was also reduced following miR-606 mimics transfection (Fig. 1C). Moreover, transfection with miR-606 mimics significantly induced the early + late apoptosis of MDA-MB-231 and BT549 cells (Fig. 1D), and miR-606-induced apoptosis was accompanied by an increase in the expression levels of cleaved-PARP, BAX and cleaved-caspase 3, and a decrease in the expression levels of the proliferative protein PCNA (Fig. 1E). To

investigate the effect of anti-miR-606 on MDA-MB-231 and BT549 TNBC cell lines, RT-qPCR analysis was performed post-transfection. The results revealed a significant reduction in miR-606 expression levels after anti-miR-606 transfection (Fig. 1F). By contrast, anti-miR-606 significantly inhibited the expression levels of apoptosis markers and induced the expression of the proliferation marker in MDA-MB-231 and BT549 cells (Fig. 1F). Collectively, these results suggested that miR-606 induces TNBC cell apoptosis.

miR-606 suppresses the sphere formation, migration and invasion of TNBC cells. Subsequently, the effects of miR-606 on various tumorigenesis-associated characteristics of TNBC cells were evaluated. It was first determined whether miR-606 influenced the preservation of the CSC-like phenotype of TNBC cells. To enrich CSC-like cells, the cells were cultured under serum-free conditions, and the self-renewal capacity of TNBC cells was investigated. The
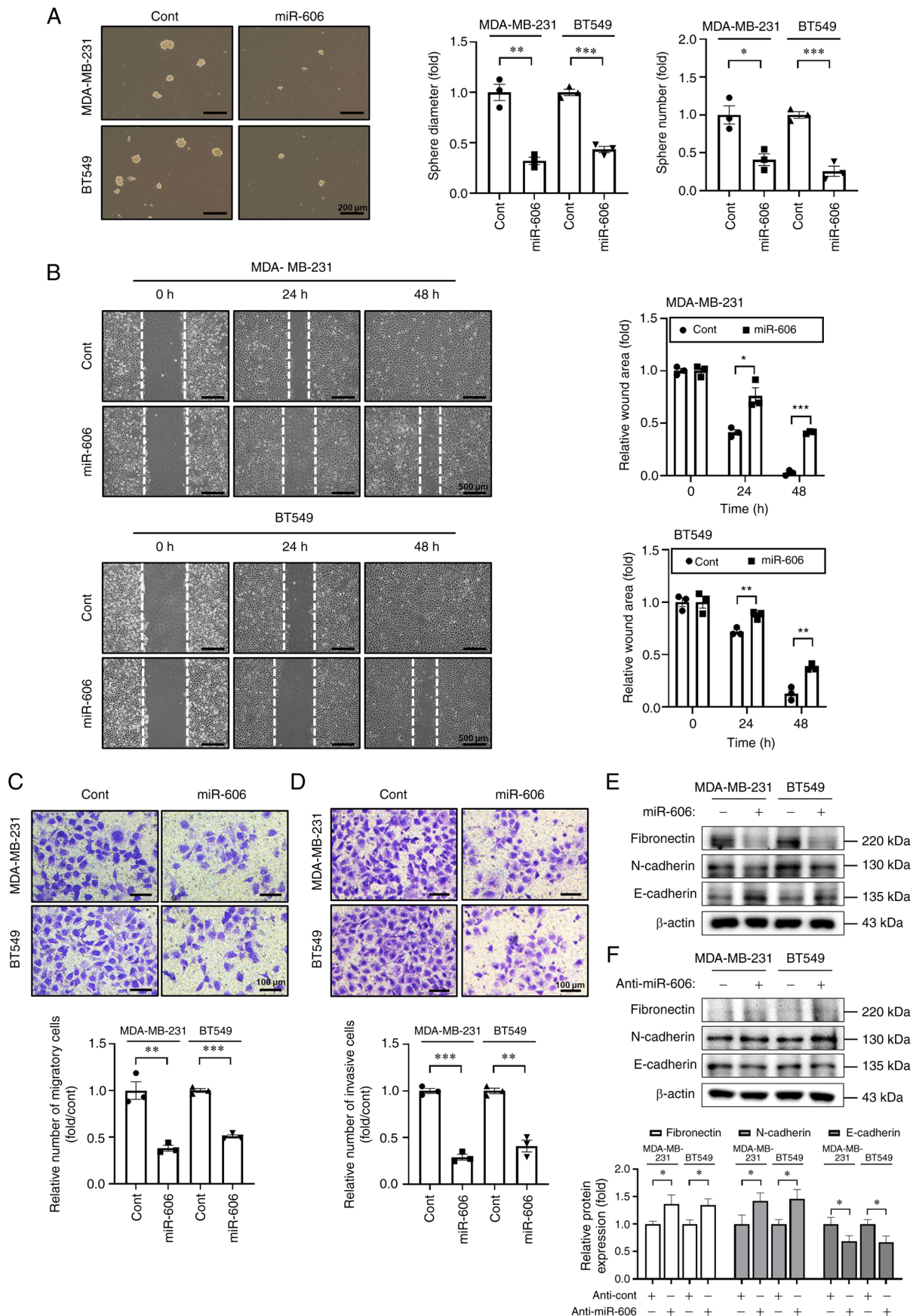
Figure 2. miR-606 inhibits the stanniogenic characteristics of TNBC cells. (A) Representative image of the sphere-forming ability of TNBC cells. The diameter and number of spheres were measured 4 days post-transfection. (B) Wound healing analysis of TNBC cells transfected with miR-606 mimics. The wound area was measured at 0, 24 and 48 h after scratching using ImageJ. Representative images of the Transwell (C) migration and (D) invasion assays. Western blot analysis of the expression levels of mesenchymal and epithelial cell marker proteins in TNBC cells transfected with (E) miR-606 mimics and (F) anti-miR-606. Data are presented as the mean ± SEM and were analyzed using Student's t-test. *P<0.05, **P<0.005 and ***P<0.001. TNBC, triple-negative breast cancer. Cont, control; miR, microRNA.
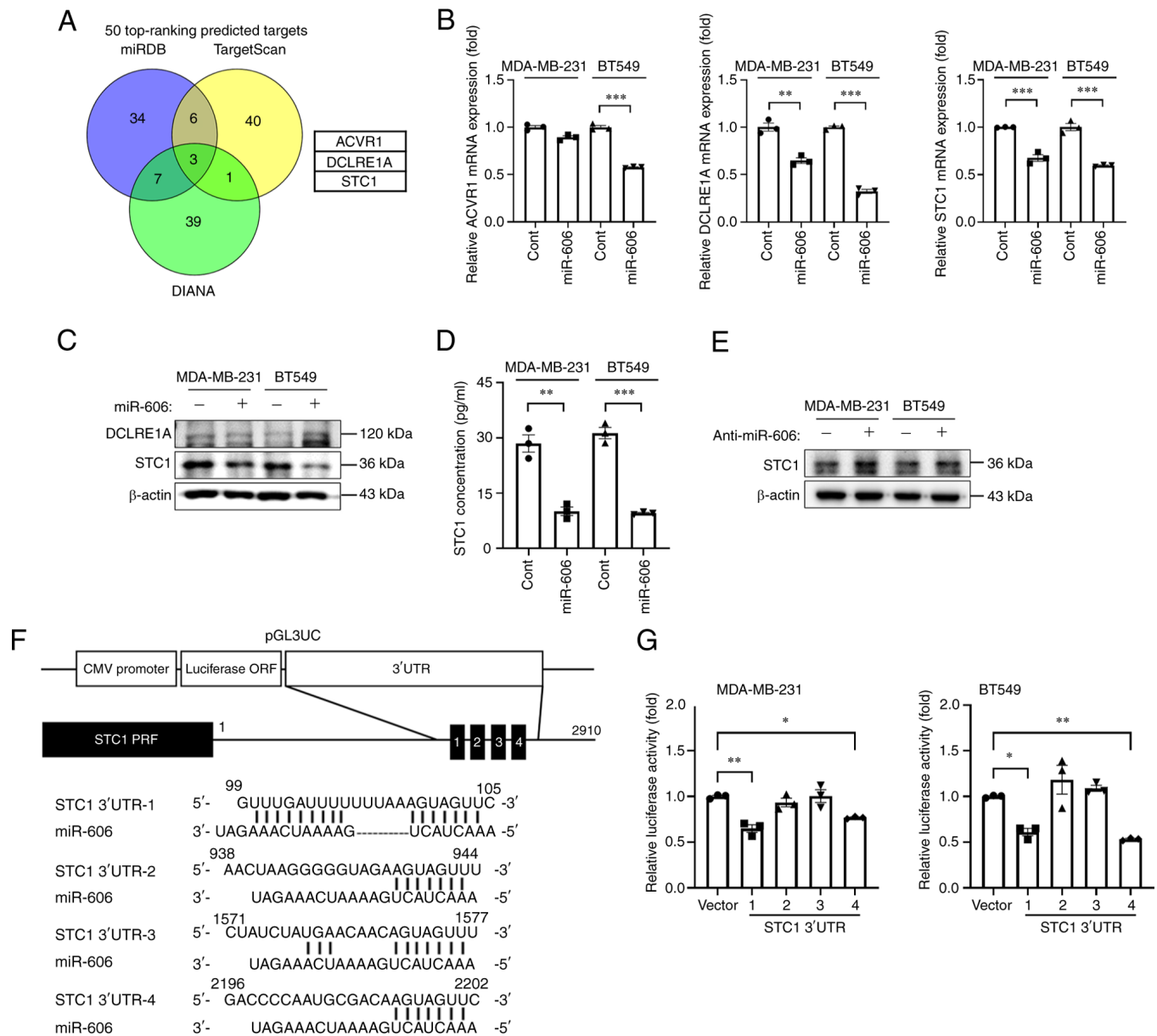
Figure 3. STC1 is a direct target gene of miR-606. (A) Venn diagram of the putative target genes of miR-606, determined using three miRNA target prediction programs. (B) Reverse transcription-quantitative PCR analysis of the relative expression levels of three putative target genes (ACVR1, DCLRE1A and STC1) in TNBC cells transfected with miR-606 mimics. (C) Western blot analysis of the protein expression levels of two putative target genes (DCLRE1A and STC1) in TNBC cells transfected with miR-606 mimics. (D) Secreted protein levels of STC1 in the supernatant of TNBC cells transfected with miR-606 mimics. (E) Protein expression levels of the target gene, STC1, in TNBC cells transfected with anti-miR-606. (F) Construction of the vector containing four putative miR-606 binding sites in the human STC1 3'-UTR. (G) Luciferase activity of TNBC cells co-transfected with the four indicated STC1 3'-UTR vectors and miR-606 mimics. Luciferase activity was measured 48 h post-co-transfection. Data are presented as the mean ± SEM. Data were analyzed using (B and D) Student's t-test and (G) one-way ANOVA. $^*P<0.05$, $^{**}P<0.005$ and $^{***}P<0.001$. TNBC, triple-negative breast cancer; ACVR1, activin A receptor, type 1; DCLRE1A, DNA cross-link repair 1A; STC1, Stanniocalcin 1; Cont, control; miR, microRNA.

tumor sphere-forming ability of MDA-MB-231 and BT549 cells in CSC-like cell growth medium was estimated 4 days after transfection with miR-606 mimics or control miRNA. It was observed that the size and number of tumor spheres were significantly decreased in cells transfected with miR-606 mimics (Fig. 2A).

Aggressive and metastatic cancer cells are characterized by enhanced cell migration and invasion. Therefore, wound healing assay, Transwell assay and western blotting were performed to determine the effects of miR-606 on the migratory and invasive abilities of TNBC cells. The results showed that transfection with miR-606 mimics significantly suppressed wound healing in MDA-MB-231 and BT549 cells (Fig. 2B). Furthermore, transfection with miR-606 mimics significantly decreased the migratory and invasive abilities of MDA-MB-231 and BT549 cells (Fig. 2C and D). Moreover, in the miR-606 mimics-transfected cells, the expression levels of the mesenchymal cell markers fibronectin and N-cadherin were downregulated, whereas those of the epithelial cell marker E-cadherin were upregulated (Fig. 2E). By contrast, in the anti-miR-606-transfected cells, the expression levels of mesenchymal cell markers
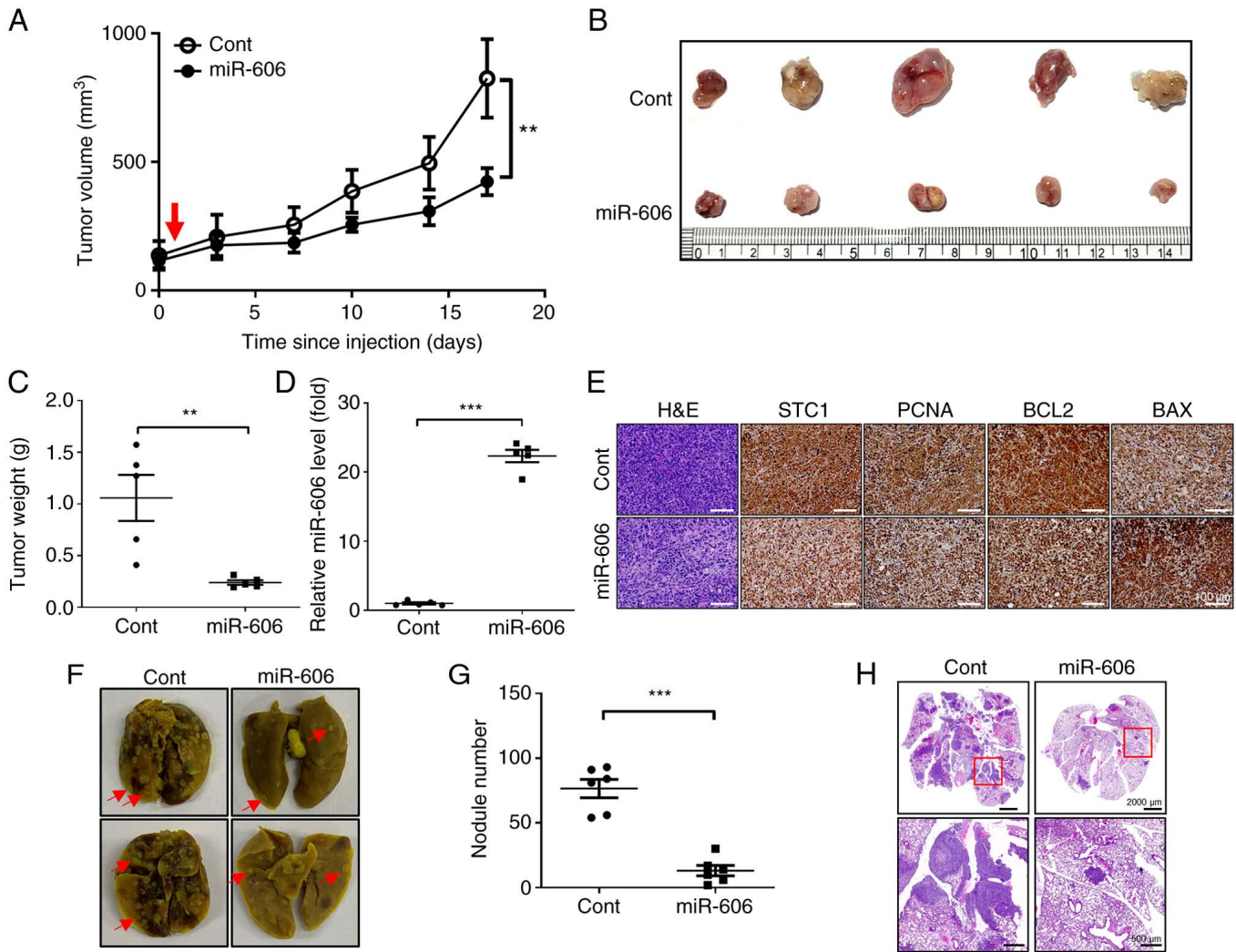
Figure 4. miR-606 suppresses tumor growth and metastasis *in vivo*. (A) Xenograft model tumor growth rate after injection at the indicated time point (red arrow) with miR-606 mimics complex. (B) Images of the resected tumor tissue of the xenograft model transfected with miR-606 mimics. (C) Comparison of tumor weight after resection. (D) Reverse transcription-quantitative PCR analysis of the relative miR-606 expression levels in resected tumor tissues transfected with miR-606 mimics. (E) Immunohistochemical analysis of tumor tissues transfected with miR-606 mimics. (F) Images of the resected lungs of mice injected with MDA-MB-231 transfected with miR-606 mimics. (G) Comparison of the nodule number in resected lung tissues injected with MDA-MB-231 cells transfected with miR-606 mimics. (H) H&E staining of resected lung tissues injected with MDA-MB-231 cells transfected with miR-606 mimics. Data are presented as the mean ± SEM and were analyzed using Student's t-test. **P<0.005 and ***P<0.001. H&E, hematoxylin and eosin; Cont, control; miR, microRNA; PCNA, proliferating cell nuclear antigen; STC1, Stanniocalcin 1.

were increased and those of the epithelial cell marker were decreased (Fig. 2F). Taken together, these results indicated that miR-606 may inhibit the tumorigenesis-associated characteristics of TNBC cells.

miR-606 directly targets STC1. The miRNA target prediction algorithms miRDB, TargetScan and DIANA were used to predict the target genes of miR-606; several candidate targets were identified (Fig. 3A). Three common genes were predicted by all three algorithms: ACVR1, DCLRE1A and STC1. Therefore, the mRNA and protein expression levels of these three target candidates were evaluated after miR-606 mimics transfection in MDA-MB-231 and BT549 cells. In both cell lines, the mRNA expression levels of DCLRE1A and STC1 were significantly downregulated in miR-606 mimics-transfected cells; however, the mRNA expression levels of ACVR1 were not significantly downregulated in miR-606

mimics-transfected MDA-MB-231 cells (Fig. 3B). Moreover, in both cell lines, the protein expression levels of STC1 were markedly reduced by miR-606 overexpression, whereas those of DCLRE1A were not altered (Fig. 3C). Additionally, it was revealed that the expression levels of STC1 were higher in TNBC cells compared with those in normal breast cells or in cell lines of other breast cancer subtypes (Fig. S3A), and the mRNA expression levels of STC1 were downregulated or upregulated in TNBC cell lines following miR-606 mimics or anti-miR-606 transfection, respectively (Fig. S3B and C). Similarly, the secreted STC1 protein levels in the supernatants of miR-606 mimics-transfected MDA-MB-231 and BT549 cells were significantly reduced compared with those in the supernatant of control miRNA-transfected MDA-MB-231 and BT549 cells (Fig. 3D). Furthermore, the protein expression levels of STC1 were increased in anti-miR-606-transfected MDA-MB-231 and BT549 cells (Fig. 3E). Therefore, STC1
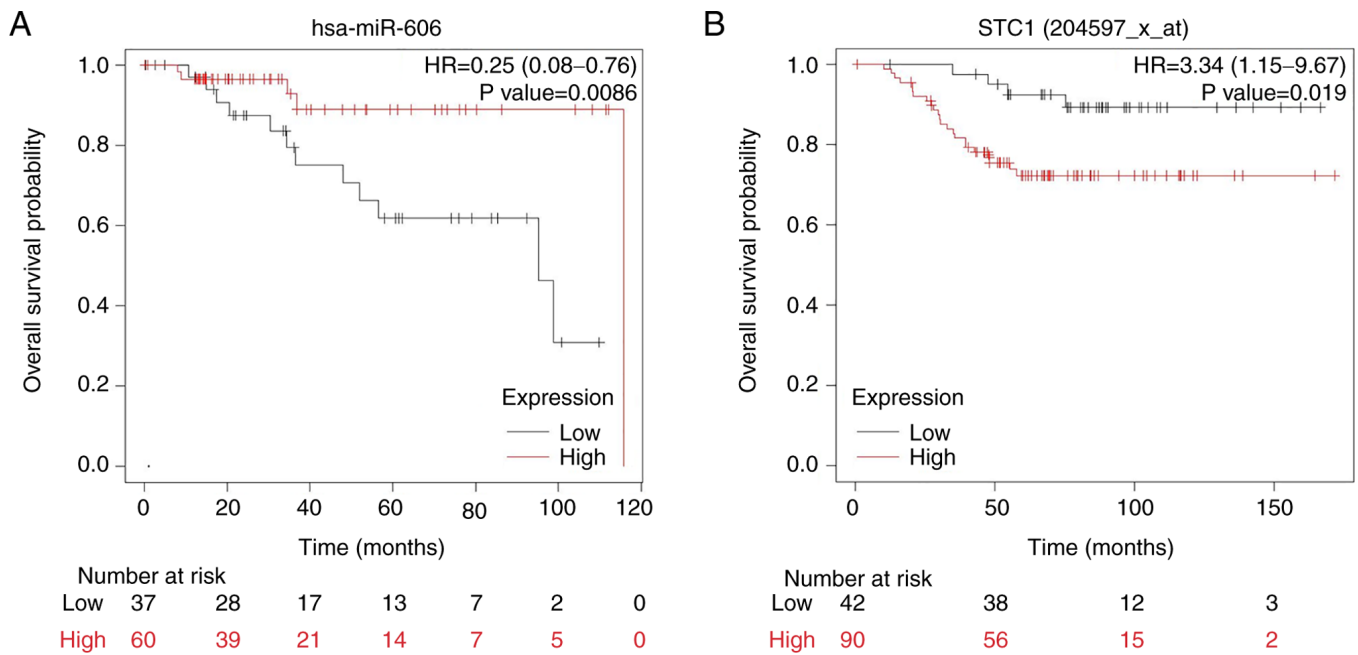
Figure 5. miR-606 and STC1 expression are associated with the OS of patients with breast cancer. Kaplan-Meier analysis of the association between (A) OS and miR-606 expression, and between (B) OS and STC1 expression in patients with breast cancer. OS, overall survival; STC1, Stanniocalcin 1; miR-microRNA.

was further investigated using a reporter assay to determine whether it is a direct target of miR-606. Four putative miR-606-binding sites, complementary to the seed region of miR-606, were identified in the 3'-UTR of STC1. Therefore, the putative miR-606-binding sequence was cloned into a modified pGL3 reporter vector, pGL3UC (Fig. 3F), and the luciferase reporter activity was measured 48 h post-co-transfection of MDA-MB-231 and BT549 cells with the reporter construct and miR-606 mimics. Co-transfection with miR-606 mimics and STC1 3'UTR-1 or -4 significantly reduced the relative luciferase activity compared with that in cells transfected with miR-606 mimics and empty pGL3UC vector (Fig. 3G). Collectively, these results indicated that STC1 is a direct target of miR-606.

miR-606 inhibits tumor growth and metastasis in a mouse xenograft model and a mouse model of lung metastasis. To confirm the tumor-suppressive effects of miR-606 *in vivo*, the changes in xenograft tumor volume were investigated after miR-606 mimics transfection. Tumors established using MDA-MB-231 cells were injected with miR-606 mimics or control miRNA alongside an *in vivo* transfection reagent. The results revealed that the tumor growth rate was significantly suppressed in mice injected with miR-606 mimics compared with that in mice injected with control miRNA (Fig. 4A). Additionally, the endpoint tumor weights of miR-606 mimics-injected mice were significantly lower than those of control miRNA-injected mice (Fig. 4B and C). The expression levels of miR-606 were also increased in the dissected tumors of mice injected with miR-606 mimics (Fig. 4D). Moreover, IHC analysis and hematoxylin and eosin staining revealed that intratumoral injections of miR-606 mimics decreased the number of tumor cells and the expression levels of the target proteins STC1, PCNA and BCL-2, but increased BAX expression (Fig. 4E).

To determine whether miR-606 inhibits metastasis *in vivo*, the number of metastatic lung nodules was detected following tail vein injection of breast cancer cell lines in a mouse model. Mouse models of lung metastasis were established by injecting control miRNA- or miR-606 mimics-transfected MDA-MB-231 cells into the tail veins of mice whose lungs were resected after 6 weeks. After lung resection, the number of metastatic nodules in the lungs of mice injected with miR-606 mimics-transfected MDA-MB-231 cells were significantly decreased compared with that in the lungs of mice injected with control miRNA-transfected MDA-MB-231 cells (Fig. 4F and G). In addition, hematoxylin and eosin staining revealed a reduction in metastatic loci in the lungs of mice injected with miR-606 mimics-transfected MDA-MB-231 cells (Fig. 4H). Taken together, these results indicated that miR-606 functions as a tumor and metastasis suppressor *in vivo*.

miR-606 and STC1 expression levels are associated with the OS of patients with TNBC. To identify the association between miR-606 and the OS of patients with TNBC, the expression profiles of 97 patients with breast cancer were analyzed from TCGA database using the K-M plotter tool. The patients were divided into high- and low-miR-606 expression groups, comprising 60 and 37 patients, respectively. Kaplan-Meier survival analysis revealed that patients with low miR-606 expression had a significantly lower OS than those with high miR-606 expression (Fig. 5A).

Furthermore, to determine the association between STC1 and the OS of patients with TNBC, the STC1 expression profiles of 132 patients with breast cancer were analyzed from TCGA database using the K-M plotter tool. The patients were divided into high- and low-STC1 expression groups, comprising 90 and 42 patients, respectively. Kaplan-Meier survival analysis revealed that patients with high STC1 expression had a significantly lower OS than those with low STC1 expression (Fig. 5B). Collectively, these results suggested that

miR-606 and STC1 may act as prognostic indicators of the OS of patients with TNBC.

Discussion

TNBC is an aggressive subtype of breast cancer with a high rate of recurrence and distant metastasis (17). Owing to the absence of ER, PR and HER2 in TNBC, currently available hormones or targeted therapies are ineffective in treating TNBC (18). Therefore, new prognostic and therapeutic biomarkers are urgently needed for the treatment of TNBC. Notably, miRNA-based therapeutics have emerged as a novel strategy for cancer treatment, since miRNAs regulate pathways associated with tumor progression and migration, and their dysregulation has been linked to various types of cancer (19,20). The potential of miRNAs as novel biomarkers has been demonstrated in various cancers, including breast cancer (21). However, the functions of several miRNAs, including the novel miR-606, remain unknown. In the present study, miR-606 was identified as a potential tumor suppressor in TNBC and STC1 was revealed to be a direct target gene of miR-606.

STC1, which was first identified in bony fish, is a 56-kDa disulfide-bound glycoprotein hormone involved in plasma calcium and phosphate homeostasis (7). Mammalian STC1 is expressed in various tissues (18) and is involved in biological processes, including mesenchymal-epithelial transition, intra-membranous and endochondral bone formation, and metabolic rate, other than calcium and phosphate homeostasis (22-24). The expression of STC-1 is altered during various developmental, physiological and pathological processes, including pregnancy, lactation, angiogenesis and apoptosis (25-27). In addition, several studies have reported the relationship between STC1 and various types of cancer. For example, STC1 overexpression has been shown to induce apoptosis in cervical cancer (23) and to mediate metastasis in colorectal cancer (28,29). Moreover, in hepatocellular carcinoma, higher STC1 expression has been associated with smaller tumor size (30).

The role of STC1 in breast cancer is complex and multifaceted (31). STC1 is associated with invasion and metastasis in TNBC cells, and high STC1 expression is associated with poor prognosis in patients with TNBC (10,32). Additionally, STC1 has been implicated in breast cancer chemoresistance (31). By contrast, in hormone receptor-positive breast cancer, high STC1 expression levels have been reported to be associated with a favorable prognosis (33). Moreover, high STC1 expression is associated with a relatively favorable prognosis in the early postoperative period, but is associated with an increased risk of breast cancer relapse in later stages (34). An association between STC1 and tumor suppression has also been established in other studies. For example, STC1 has been shown to be associated with BRCA1, a tumor suppressor gene in breast cancer (24). Additionally, STC1 can influence components of the tumor microenvironment, such as cancer-associated fibroblasts (35).

In the present study, miR-606 was identified as a miRNA with tumor-suppressive properties in TNBC. The results of the present study demonstrated that miR-606 could effectively target and inhibit the activity of the STC1 gene, thus exhibiting anticancer effects both *in vitro* and *in vivo*. Furthermore, to validate the findings of the current study, an analysis was conducted using publicly available databases. This analysis confirmed that in patients with TNBC elevated STC1 expression levels and reduced miR-606 levels resulted in shorter OS rates. Notably, the present clinical analysis had a limitation, as it did not explore inverse relationship between miR-606 and STC1 within the same group of patients.

In conclusion, the findings of the present study revealed that miR-606 may inhibit TNBC cell proliferation, stem cell-like ability, migration and invasion by targeting STC1. Consequently, it could act as a tumor and metastasis suppressor, suggesting its potential in the development of anticancer miRNA therapeutics, particularly for TNBC.

Availability of data and materials

The datasets used and/or analyzed during the current study are available from the corresponding author on reasonable request. The datasets generated and/or analyzed during the current study are available in the GSE118782 repository, https://www.ncbi.nlm.nih.gov/geo/query/acc.cgi?acc=GSE118782.

Authors' contributions

IK and SL made substantial contributions to conception and design, and contributed to manuscript review, funding acquisition, investigation and methodology. SC was involved in experiments, acquisition of the data, interpretation of the data and writing of the original draft. HJA was involved in experiments, acquisition of the data, interpretation of the data, writing of the original draft and project administration. HJY and MJS were involved in experiments and formal analysis. JO, KL and SAL were involved in analysis of data, and reviewing and editing of the manuscript. SKK and JK were involved in acquisition and analysis of data. IK and SL confirmed the authenticity of all the raw data. All authors read and approved the final manuscript.

Ethics approval and consent to participate

Animal experimental procedures were reviewed and approved by the CHA University Animal Care and Use Committee (approval no. 210152).

Patient consent for publication

Not applicable.

Competing interests

The authors declare that they have no competing interests.

References

1. Siegel RL, Miller KD, Fuchs HE and Jemal A: Cancer statistics, 2022. CA Cancer J Clin 72: 7-33, 2022.
2. Sørlie T, Perou CM, Tibshirani R, Aas T, Geisler S, Johnsen H, Hastie T, Eisen MB, Van De Rijn M, Jeffrey SS, et al: Gene expression patterns of breast carcinomas distinguish tumor subclasses with clinical implications. Proc Natl Acad Sci USA 98: 10869-10874, 2001.
3. Foulkes WD, Smith IE and Reis-Filho JS: Triple-negative breast cancer. N Engl J Med 363: 1938-1948, 2010.
4. Takahashi RU, Miyazaki H and Ochiya T: The roles of microRNAs in breast cancer. Cancers (Basel) 7: 598-616, 2015.
5. Ding L, Gu H, Xiong X, Ao H, Cao J, Lin W, Yu M, Lin J and Cui Q: MicroRNAs involved in carcinogenesis, prognosis, therapeutic resistance and applications in human triple-negative breast cancer. Cells 8: 1492, 2019.
6. Loh HY, Norman BP, Lai KS, Rahman NMANA, Alitheen NBM and Osman MA: The regulatory role of microRNAs in breast cancer. Int J Mol Sci 20: 4940, 2019.
7. Yoshiko Y and Aubin JE: Stanniocalcin 1 as a pleiotropic factor in mammals. Peptides 25: 1663-1669, 2004.
8. Lin F, Li X, Wang X, Sun H, Wang Z and Wang X: Stanniocalcin 1 promotes metastasis, lipid metabolism and cisplatin chemoresistance via the FOXC2/ITGB6 signaling axis in ovarian cancer. J Exp Clin Cancer Res 41: 129, 2022.
9. Bai S, Zhao Y, Chen W, Peng W, Wang Y, Xiong S, Aruna, Li Y, Yang Y, Chen S, et al: The stromal-tumor amplifying STC1-Notch1 feedforward signal promotes the stemness of hepatocellular carcinoma. J Transl Med 21: 236, 2023.
10. Chang AC, Doherty J, Huschtscha LI, Redvers R, Restall C, Reddel RR and Anderson RL: STC1 expression is associated with tumor growth and metastasis in breast cancer. Clin Exp Metastasis 32: 15-27, 2015.
11. Liu A, Li Y, Lu S, Cai C, Zou F and Meng X: Stanniocalcin 1 promotes lung metastasis of breast cancer by enhancing EGFR-ERK-S100A4 signaling. Cell Death Dis 14: 395, 2023.
12. Chandran UR, Medvedeva OP, Barmada MM, Blood PD, Chakka A, Luthra S, Ferreira A, Wong KF, Lee AV, Zhang Z, et al: TCGA expedition: A data acquisition and management system for TCGA data. PLoS One 11: e0165395, 2016.
13. Barrett T, Wilhite SE, Ledoux P, Evangelista C, Kim IF, Tomashevsky M, Marshall KA, Phillippy KH, Sherman PM, Holko M, et al: NCBI GEO: Archive for functional genomics data sets-update. Nucleic Acids Res 41: D991-D995, 2013.
14. Lasham A, Fitzgerald SJ, Knowlton N, Robb T, Tsai P, Black MA, Williams L, Mehta SY, Harris G, Shelling AN, et al: A predictor of early disease recurrence in patients with breast cancer using a cell-free RNA and protein liquid biopsy. Clin Breast Cancer 20: 108-116, 2020.
15. Livak KJ and Schmittgen TD: Analysis of relative gene expression data using real-time quantitative PCR and the 2(-Delta Delta C(T)) method. Methods 25: 402-408, 2001.
16. Wang H, Zhang W, Ding Z, Xu T, Zhang X and Xu K: Comprehensive exploration of the expression and prognostic value of AQPs in clear cell renal cell carcinoma. Medicine (Baltimore) 101: e29344, 2022.
17. Yao Y, Chu Y, Xu B, Hu Q and Song Q: Risk factors for distant metastasis of patients with primary triple-negative breast cancer. Biosci Rep 39: BSR20190288, 2019.
18. De Laurentiis M, Cianniello D, Caputo R, Stanzione B, Arpino G, Cinieri S, Lorusso V and De Placido S: Treatment of triple negative breast cancer (TNBC): Current options and future perspectives. Cancer Treat Rev 36 (Suppl 3): S80-S86, 2010.
19. Wu M, Wang G, Tian W, Deng Y and Xu Y: MiRNA-based therapeutics for lung cancer. Curr Pharm Des 23: 5989-5996, 2018.
20. Mishra S, Yadav T and Rani V: Exploring miRNA based approaches in cancer diagnostics and therapeutics. Crit Rev Oncol Hematol 98: 12-23, 2016.
21. Heneghan HM, Miller N, Lowery AJ, Sweeney KJ, Newell J and Kerin MJ: Circulating microRNAs as novel minimally invasive biomarkers for breast cancer. Ann Surg 251: 499-505, 2010.
22. Chang AC, Jeffrey KJ, Tokutake Y, Shimamoto A, Neumann AA, Dunham MA, Cha J, Sugawara M, Furuichi Y and Reddel RR: Human stanniocalcin (STC): Genomic structure, chromosomal localization, and the presence of CAG trinucleotide repeats. Genomics 47: 393-398, 1998.
23. Madsen KL, Tavernini MM, Yachimec C, Mendrick DL, Alfonso PJ, Buergin M, Olsen HS, Antonaccio MJ, Thomson AB and Fedorak RN: Stanniocalcin: A novel protein regulating calcium and phosphate transport across mammalian intestine. Am J Physiol 274: G96-G102, 1998.
24. Chang AC, Jellinek DA and Reddel RR: Mammalian stanniocalcins and cancer. Endocr Relat Cancer 10: 359-373, 2003.
25. Deol HK, Varghese R, Wagner GF and Dimattia GE: Dynamic regulation of mouse ovarian stanniocalcin expression during gestation and lactation. Endocrinology 141: 3412-3421, 2000.
26. Zlot C, Ingle G, Hongo J, Yang S, Sheng Z, Schwall R, Paoni N, Wang F, Peale FV Jr and Gerritsen ME: Stanniocalcin 1 is an autocrine modulator of endothelial angiogenic responses to hepatocyte growth factor. J Biol Chem 278: 47654-47659, 2003.
27. Block GJ, Ohkouchi S, Fung F, Frenkel J, Gregory C, Pochampally R, DiMattia G, Sullivan DE and Prockop DJ: Multipotent stromal cells are activated to reduce apoptosis in part by upregulation and secretion of stanniocalcin-1. Stem Cells 27: 670-681, 2009.
28. Pan X, Jiang B, Liu J, Ding J, Li Y, Sun R, Peng L, Qin C, Fang S and Li G: STC1 promotes cell apoptosis via NF-κB phospho-P65 Ser536 in cervical cancer cells. Oncotarget 8: 46249-46261, 2017.
29. Peña C, Céspedes MV, Lindh MB, Kiflemariam S, Mezheyeuski A, Edqvist PH, Hägglöf C, Birgisson H, Bojmar L, Jirström K, et al: STC1 expression by cancer-associated fibroblasts drives metastasis of colorectal cancer. Cancer Res 73: 1287-1297, 2013.
30. Leung CC and Wong CK: Effects of STC1 overexpression on tumorigenicity and metabolism of hepatocellular carcinoma. Oncotarget 9: 6852-6861, 2017.
31. Chen F, Zhang Z and Pu F: Role of stanniocalcin-1 in breast cancer. Oncol Lett 18: 3946-3953, 2019.
32. Murai R, Tanaka M, Takahashi Y, Kuribayashi K, Kobayashi D and Watanabe N: Stanniocalcin-1 promotes metastasis in a human breast cancer cell line through activation of PI3K. Clin Exp Metastasis 31: 787-794, 2014.
33. McCudden CR, Majewski A, Chakrabarti S and Wagner GF: Co-localization of stanniocalcin-1 ligand and receptor in human breast carcinomas. Mol Cell Endocrinol 213: 167-172, 2004.
34. Joensuu K, Heikkilä P and Andersson LC: Tumor dormancy: Elevated expression of stanniocalcins in late relapsing breast cancer. Cancer Lett 265: 76-83, 2008.
35. Avalle L, Raggi L, Monteleone E, Savino A, Viavattene D, Statello L, Camperi A, Stabile SA, Salemme V, De Marzo N, et al: STAT3 induces breast cancer growth via ANGPTL4, MMP13 and STC1 secretion by cancer associated fibroblasts. Oncogene 41: 1456-1467, 2022.